


Influence of force causing water molecules to flow in computer simulations of water nanoflows

Janusz BYTNAR¹ , Bogusław TWARÓG², Kamil SZOSTEK³, and Monika PIRÓG¹

¹ Faculty of Technical Engineering, State University of Applied Sciences in Jarosław, ul. Czarnieckiego 16, Jarosław, 37-500, Poland

² Institute of Computer Science, University of Rzeszów, ul. Pigonia 1, Rzeszów, 35-959, Poland

³ Department of Electrical and Computer Engineering Fundamentals, Rzeszów University of Technology, ul. Pola 2, 35-959 Rzeszów, Poland

Abstract. Understanding liquid behavior in nanoscale channels is essential for designing advanced systems involving nanofluids. The objective of this study was to evaluate the effect of external forcing applied to water molecules flowing through a copper nanochannel on the thermodynamic stability of the system, using molecular dynamics (MD) simulations. The motivation stems from the lack of clear guidelines for selecting forcing parameters that ensure physically consistent flow without introducing artificial phase transitions. Simulations were conducted for three molecular water models (OPC, PPC, TIP4P) and three forcing magnitudes. The temperature evolution and molecular velocity distributions were analyzed. The results demonstrate that excessive forcing leads to nonphysical behavior, such as overheating beyond the boiling point, whereas insufficient forcing may cause cooling below the freezing point. Only intermediate forcing values allow for stable, realistic flow behavior within the liquid phase. Additionally, the choice of molecular water model was shown to significantly affect flow dynamics, highlighting the importance of proper parameter selection in MD studies. These findings provide practical guidelines for reliable nanoscale flow simulations and may support the design of transport structures in nanoscale devices.

Keywords: computer simulation; molecular dynamics; nanoflows.

1. INTRODUCTION

Recent years have seen a significant increase in the use of computer simulations in nanotechnology research: genetics, bioinformatics, nanomechanics, materials engineering, etc. [1–3]. Today, computer simulations often replace laboratory experiments, which are often unavailable in the case of nanotechnology. Furthermore, thanks to computer simulations of nanophenomena, it is possible to design the processes studied with much greater accuracy and reproducibility than with experimental techniques on such a small scale. These include research on nanomaterials, biomachines, nanoemulsions, nanogenetics, and nanofluidics [2, 4, 5].

Conducting a computer simulation of a real process requires building an appropriate mathematical model of that process. A computational model, which is a discretized approximation of the mathematical model, is then created to allow computer implementation [6].

One method that enables nanoscale calculations is molecular dynamics (MD), based on replacing real matter with molecular models. To obtain accurate and reliable simulation results of real processes, it is necessary to select the relevant algorithms, key in MD, and the right parameters to ensure the thermodynamic stability of the system. In addition, appropriate molecular

models of the materials must be selected, as well as appropriate methods for performing intermolecular interactions (interaction potentials).

For computer simulations based on the molecular dynamics method, reducing computational complexity (including simulation time and memory reservation) is a critical issue. This is related to determining the instantaneous positions of the molecules and calculating the interactions of each pair of molecules. If computational simplification mechanisms are not applied, the complexity is of the order of N^2 (where N is the number of molecules in the simulated system), because the calculation of the interactions between each pair of molecules must be performed twice [7].

On the other hand, in the case of molecular dynamics simulation of real processes, it is crucial to maintain the simulated system in thermodynamic equilibrium. This is a key concern in the case of dynamic processes, where forced movement of molecules can lead to a change in the state of aggregation of the simulated medium.

Computer simulations of real processes by MD require the use of appropriate molecular models of substances. Different molecular models can be applied to some real matter. An example is water, whose molecular models can be found in papers [8, 9]. The possibility of choosing these models in the MD method can sometimes produce inappropriate simulation results, such as a change in the state of aggregation of the simulated medium – water. This study aims to evaluate the impact of the forcing strength used to drive water molecule flow in a nanochannel on the reliability of replicating real flow phenom-

*e-mail: janusz.bytnar@pansjar.edu.pl

Manuscript submitted 2025-03-11, revised 2025-12-04, initially accepted for publication 2025-12-09, published in March 2026.

ena at the nanometer scale. The analysis focuses on determining the extent to which forcing mechanisms employed in numerical models may distort the characteristics of actual liquid transport in nanochannels. Although a similar issue was addressed in [10], the influence of different forcing methods was not considered. This article focuses on identifying the conditions under which real flow behavior deviates from model predictions, especially in the context of phase transitions of the liquid into solid or gaseous states. Additionally, the use of three molecular models of water enables a comprehensive assessment of how the adopted molecular representation affects flow dynamics at the nanoscale.

2. MOLECULAR MODEL OF MATERIALS AND MODELS OF INTERMOLECULAR INTERACTIONS

The structure of the water molecule (Fig. 1a) is relatively complex and can only be accurately described in the framework

of quantum mechanics. However, this kind of description does not apply to molecular dynamics simulation; therefore, several simplified models are proposed.

As mentioned above, simulating real processes at the molecular level requires the use of appropriate molecular models of real substance. When molecular models are used, it is important to bear in mind that their inaccurate description may result in some deviations from the properties of the real substance. Furthermore, for some real matter, such as water, there are many different molecular models (see Table 1) [8]. Individual models may differ in charge distribution, mass, geometry of the molecule structure, and Lennard-Jones potential parameters. Molecular dynamics requires a description of the molecules and the forces acting between them. The Lennard-Jones potential is one of the most widely used models for describing forces [1, 11, 12] (see Fig. 2). It assumes spherically symmetric molecules that repel each other at short distances and attract each other at longer distances.

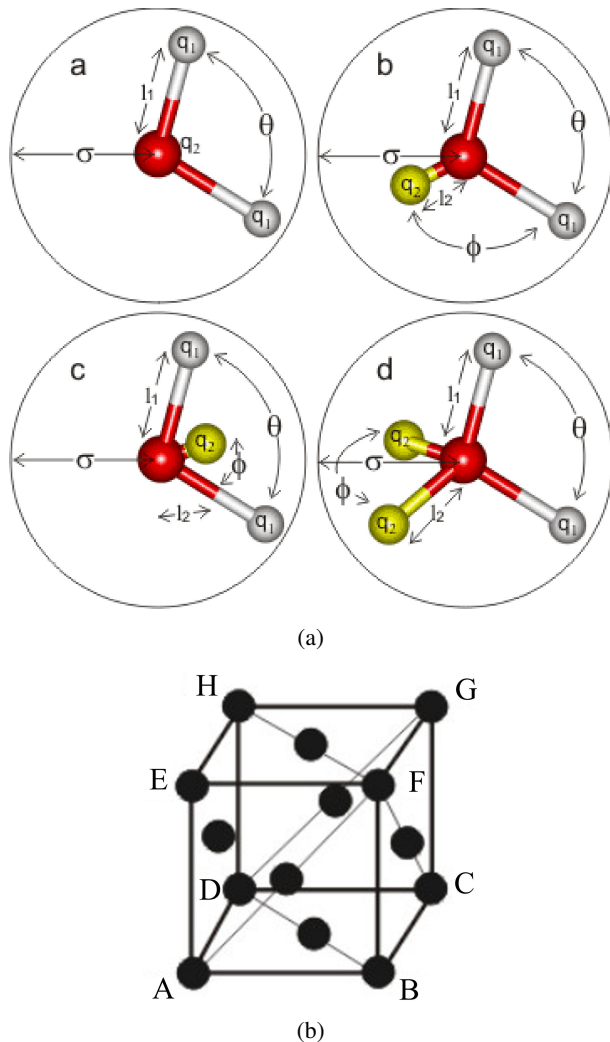


Fig. 1. Molecular models of materials: geometrical models of a water molecule (a) [8]: l_1 – distance of q_1 charges from oxygen atom, l_2 – distance of q_2 charges from oxygen atom, σ – Lennard-Jones potential constant, ϕ – angle between q_2 charges, θ – angle between q_1 charges); elementary copper crystal (14 copper atoms) (b)

Table 1

Models of molecular water parameters used in simulations [8]

Model	Geometrical configuration (Fig. 1a)	Lennard-Jones molecular analysis diameter σ $1 \cdot 10^{-10}$ m	Lennard-Jones potential well depth ε kJ/mol	$l_1, 1 \cdot 10^{-10}$ m	$l_2, 1 \cdot 10^{-10}$ m
OPC	<i>c</i>	3.1666	0.8903	0.8724	0.1594
PPC	<i>b</i>	3.23400	0.6000	0.9430	0.0600
TIP4P	<i>c</i>	3.15365	0.6480	0.9572	0.1500

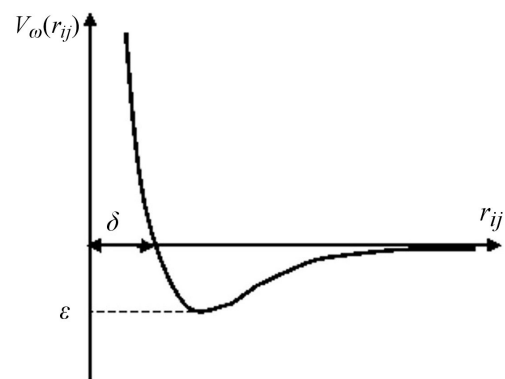


Fig. 2. Lennard-Jones potential used in simulations (r_{ij} – interatomic distance)

The most common form of this potential is as follows:

$$V_{LJ}(r) = 4\varepsilon \left[\left(\frac{\sigma}{r_{\alpha\beta}} \right)^{12} - \left(\frac{\sigma}{r_{\alpha\beta}} \right)^6 \right], \quad (1)$$

where $r_{\alpha\beta}$ – distance between atoms, ε – the potential depth [kJ/mol], δ – the distance between the centers of mass of

atoms at which the potential becomes zero, usually expressed in angstroms [\AA].

A molecular dynamics simulation can be divided into several key stages:

- Starting point – initial coordinates for the molecules based on one of the crystal lattice models, initial velocities from Maxwell-Boltzman distribution.
- Creating lists of neighboring molecules – selection of molecules for intermolecular interactions.
- Calculation of forces – calculate the total force on each particle:

$$F_i = \sum_j F_{ij}. \quad (2)$$

- Solution of equations – Newton's integral equations of motion for each molecule:

$$\frac{d^2 r_i}{dt^2} = \frac{F_i}{m_i}. \quad (3)$$

- Motion of molecules – determination of new positions $r_i(t)$ and velocities $v_i(t)$ for each molecule:

$$\begin{aligned} r_i(t) &\rightarrow r_i(t + \Delta t), \\ v_i(t) &\rightarrow v_i(t + \Delta t). \end{aligned} \quad (4)$$

In molecular dynamics, we follow the laws of classical mechanics:

$$F_i = m_i * a_i \quad (5)$$

for each atom i in the system constituted by N atoms. Here m_i is the atom mass,

$$a_i = \frac{d^2 r_i}{dt^2} \quad (6)$$

its acceleration, and F_i the force acting upon it, due to the interactions with other atoms.

The motion is governed by the Newton-Euler equations:

$$M_i \ddot{R}_i = F_i + F_x^*, \quad (7)$$

where M_i is the total mass of molecule i , R_i is the center of mass of molecule i , F_i is the total force acting on molecule i , F_x^* is the mass force necessary to set water in motion.

Simulations were performed using the Moldy program [13], suitably modified to force water molecules to flow in the nanochannel. Moldy is a computer program for performing molecular dynamics simulations of condensed matter. It is free software, which may be redistributed and/or modified under the terms of the GNU.

To set water in motion, a mass force F_x^* (see Fig. 3 and equation (7)), directed along the X -axis, in the positive direction, was applied to every water molecule.

Simulations were conducted for three molecular models of water and three values of driving force for water molecules in a copper nanochannel. The width of the nanochannel was equal to about 5 water molecule diameters (see Fig. 3).

The molecular parameters of the materials were taken from the literature (see Table 1) [8]. The geometry of the molecular

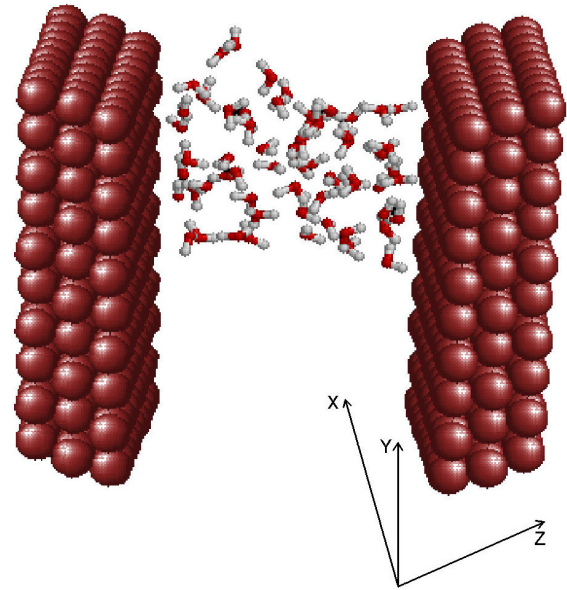


Fig. 3. View of the water/copper elementary cell used for the simulation – picture made with the Moldy program [13]

models of water and copper is shown in Fig. 1. According to the assumed molecular models, the interactions between water molecules, as well as water and wall molecules, were described with the Lennard-Jones potential [8, 14, 15].

In the simulations performed, the elementary cell was in the form of a cuboid and contained water molecules surrounded by a wall of copper atoms (see Fig. 3). Each wall consisted of $10 * 10 * 3$ copper atoms. Simulations were conducted for 60 and 280 water molecules. For greater transparency, not all the walls of the channel are included in Fig. 3. In reality, the water molecules were surrounded by four walls using a symmetric reflection of the copper wall. Only in the direction of flow (X -axis) was space left for water molecules.

In these studies, a Gaussian thermostat was used for the initial 10000 time steps. Due to the interference of thermostats in the dynamics of the system, their use is recommended only in the initial phase, until thermodynamic equilibrium is achieved [11]. After this phase, any temperature fluctuations, also resulting from numerical errors, can be controlled by selected algorithms, although their overuse should be avoided due to the risk of introducing nonphysical effects into molecular dynamics [13].

In MD simulations, physical quantities are usually given in rescaled units [7, 11] (Table 2), i.e., related to m , where m is the molecular weight of the molecule, δ and ε are the characteristic parameters of the Lennard-Jones potential (see Fig. 2, equation (1) and Table 1).

Their values are marked with an asterisk [16]. Dimensionless units provide several computational benefits, such as numerical values close to unity and simplifying the equations of motion. However, the most useful benefit of using dimensionless units is that a single model represented in dimensionless units can be scaled for different problems [10].

Table 2

Reduced units of characteristic quantities using the Lennard-Jones potential in MD simulations

Time τ^*	Numerical density n^*	Temperature T^*	Velocity V_x^*	Force F_x^*
$\delta^{-1}(m/\varepsilon)^{-1/2}t$	$(N\delta^3)/v$	$k_B/\varepsilon T$	$V_x(\varepsilon/m)^{1/2}$	$F\delta/\varepsilon$

where k_B – Boltzmann constant, N – number of molecules, v – the cell volume, m – molecular mass of the molecule

3. RESULTS

The results relate to the temperature of the medium (water) and the velocity distribution in a nanochannel (made of copper atoms) for three molecular models of water: OPC, PPC, TIP4P, with the corresponding parameters (Table 1). The molecular parameters of copper were taken from [17]. In addition, the actual density and molecular weight of water and copper were taken into account when building the elementary calculation cell. The width of the copper channel, in which the dynamic flow of the water molecules was forced, was 5 water molecule diameters. 300 K was taken as the temperature of the medium. To set water in motion, a mass force F_x^* was applied to every water molecule. Three force values were selected: 0.5, 2.5, and 5.0. These F_x^* values are rescaled values as described in Table 2.

Temperature graphs were made from data stored in temporary collections during simulation. Graphs of hydrodynamic flow quantities (velocity distribution V_x^* – see Table 2) in the channel were also prepared based on data collected in the instantaneous sets that were recorded there during the simulation run (100 000 time steps of $\Delta t = 0.5$ fs). These data were averaged using a histogram-based layered method, which was used to calculate macroscopic flow quantities in the paper [18].

Figure 4 presents a graph of water temperature during simulation for the OPC molecular model of water. It compares three temperature plots for different values of the force that drives water molecules in the nanochannel. The diagram also shows two planes that define the change in the state of aggregation of water (gas and ice).

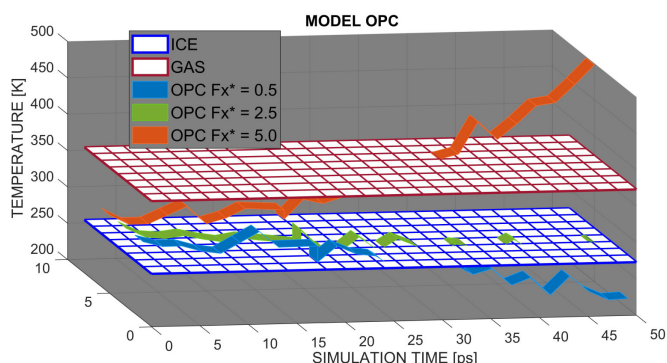


Fig. 4. Temperature of the water (60 molecules of water – model OPC) – various forces driving the flow

In the diagram presented, it can be seen that a higher force ($F_x^* = 5.0$) driving the flow of water molecules causes the temper-

ature to rise above 373 K at the end of the simulation. The water, therefore, changes to a gaseous state. In contrast, in the case of a smaller force ($F_x^* = 0.5$), the water temperature drops below 273 K. In this case, water changes its state of aggregation to solid.

An explanation for the above temperature plots can be provided by the velocity distribution of water molecules in the nanochannel at the beginning and final stages of the simulation, shown in Figs. 5 and 6. Comparing the velocity distribution in the initial (Fig. 5) and final (Fig. 6) phases of the simulation, one can notice an increase in the velocity of water molecules during the simulation, which may cause its temperature to increase. Only in the case of a small force ($F_x^* = 0.5$), does the velocity of the molecules in the nanochannel not increase.

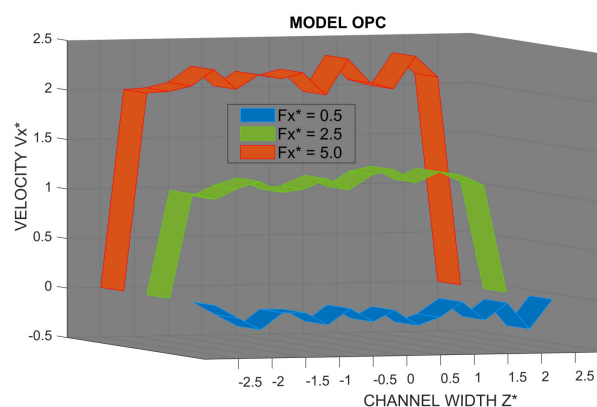


Fig. 5. Velocity distribution in a copper nanochannel in the direction of flow (60 molecules of water – model OPC, time interval 5–30 ps)

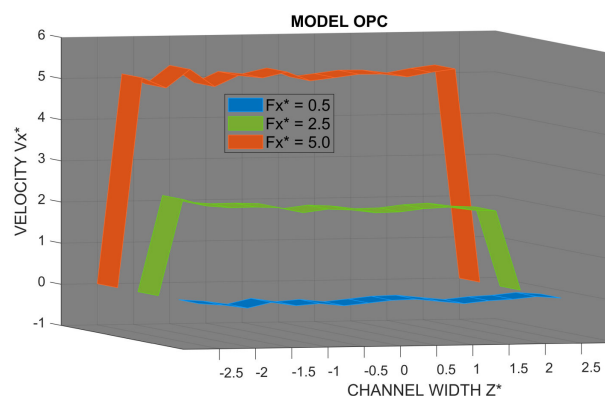


Fig. 6. Velocity distribution in a copper nanochannel in the direction of flow (60 molecules of water – model OPC, time interval 30–50 ps)

Figure 7 presents a graph of water temperature during simulation for the PPC molecular model of water. It compares three temperature plots for different values of the force that drives the flow of water molecules in the nanochannel.

Using this molecular model of water (PPC), it was observed that a higher force ($F_x^* = 5.0$) driving water molecules to flow in the nanochannel causes a rapid increase in temperature during simulation. In this case, the water changes to a gaseous state.

Influence of force causing water molecules to flow in computer simulations of water nanoflows

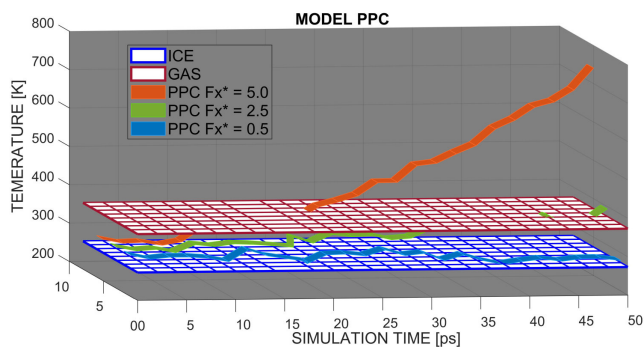


Fig. 7. Temperature of the water (60 molecules of water – model PPC) – various forces driving the flow

When a smaller force ($F_x^* = 2.5$ and $F_x^* = 0.5$) is applied, the temperature of the medium (water) is stable and does not change its aggregation state.

Confirmation of the temperature results obtained can be provided by graphs of the velocity distribution in the nanochannel (Figs. 8 and 9). With the applying of force ($F_x^* = 5.0$ and $F_x^* = 2.5$), the velocity of the water molecules increases twice at the end of the simulation (30–50 ps, see Fig. 9) compared

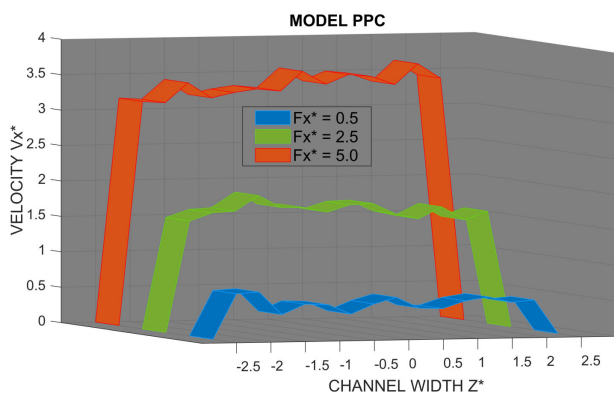


Fig. 8. Velocity distribution in a copper nanochannel in the direction of flow (60 molecules of water – model PPC, time interval 5–30 ps)

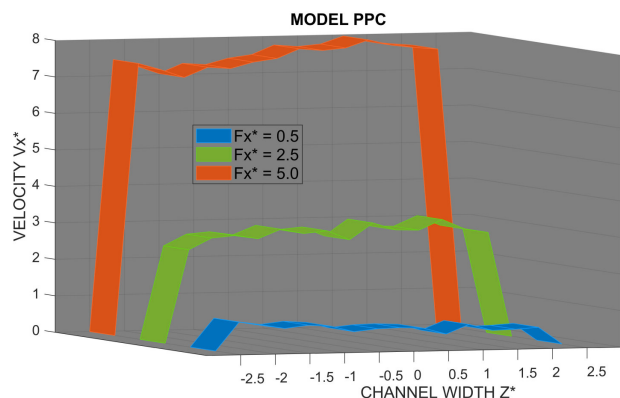


Fig. 9. Velocity distribution in a copper nanochannel in the direction of flow (60 molecules of water – model PPC, time interval 30–50 ps)

to the velocity of the water molecules during the first phase of the simulation (5–30 ps, see Fig. 8). When force ($F_x^* = 0.5$) is applied, the velocity of the water molecules remains stable.

Figure 10 presents a graph of water temperature during simulation for the TIP4P molecular model of water. It compares three temperature plots for different values of the force that drives the flow of water molecules in the nanochannel. Using this molecular model of water (TIP4P), remarkably similar results can be observed for the temperature of the medium (water) during simulation, as well as results for the velocity distribution of water molecules in a nanochannel made of copper atoms.

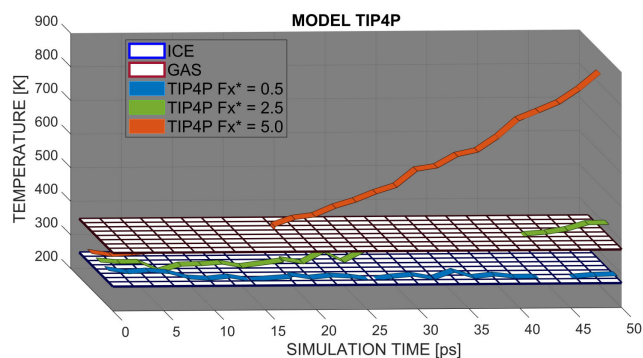


Fig. 10. Temperature of the water (60 molecules of water – model TIP4P) – various forces driving the flow

The use of a larger force ($F_x^* = 5.0$) driving the water molecules to flow, also in this case, causes the temperature of the medium (water) to rise above 373 K, resulting in a transition to a gaseous state of aggregation. The use of force ($F_x^* = 2.5$) allows for a stable temperature, but at the very end of the simulation, water also changes to a gaseous state. Only by using a smaller force ($F_x^* = 0.5$) can a stable water temperature be achieved during the entire simulation.

Figures of the water velocity distributions in the nanochannel for the TIP4P model (Figs. 11 and 12) for the initial and final phases of the simulation show a significant increase in the velocity of water molecules during the entire simulation with force ($F_x^* = 5.0$ and $F_x^* = 2.5$). With force ($F_x^* = 0.5$), the velocity distribution of water molecules in the nanochannel remains stable.

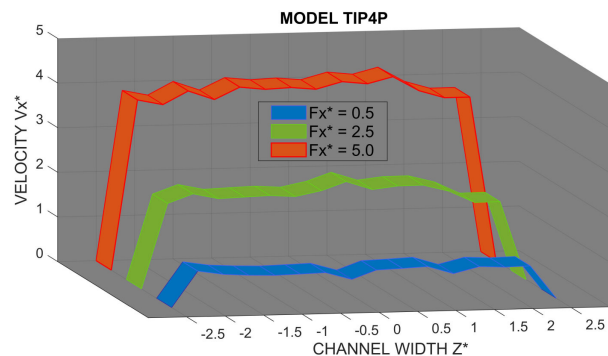


Fig. 11. Velocity distribution in a copper nanochannel in the direction of flow (60 molecules of water – model TIP4P, time interval 5–30 ps)

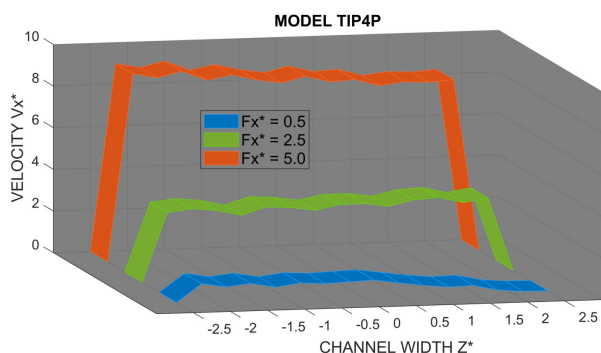


Fig. 12. Velocity distribution in a copper nanochannel in the direction of flow (60 molecules of water – model TIP4P, time interval 30–50 ps)

The simulation results were compared with the experimental results available on water flow in nanochannels. Particular attention was given to studies in which mass or volume flux was measured directly in channels of comparable geometrical dimensions ($\sim 1\text{--}10\text{ nm}$), for example, using techniques such as:

- Nano-PIV (particle image velocimetry)
- NMR microfluidic flow measurements
- Mass flowmetry at nanoscales

These experiments (e.g., Whitby & Quirke, *Nature Nanotechnology*, 2007 [19]; Majumder *et al.*, *Nature*, 2005 [20]) showed that the water flow in nanochannels significantly deviates from the predictions of the classical Poiseuille law due to the slipping effect and low flow resistance, among others.

The mass flux of water obtained under these conditions corresponds to values on the order of 10^{-15} to 10^{-12} kg/s, depending on the length of the channel, pressure, and wall material. Comparing these data with the results obtained in the simulations (after rescaling the results expressed in reduced units), it was observed that the order of magnitude of the flux is consistent when medium driving forces are used ($F_x^* = 0.5\text{--}2.5$), while higher forces ($F_x^* = 5.0$) lead to a significant increase in velocity and temperature, which in practice would correspond to

nonphysical experimental conditions (e.g., local evaporation or superheating) (Table 3).

Notes and interpretation:

- Values estimated from V_x^* data and temperature distributions, are within the typical range of simulation and experimental results on $< 10\text{ nm}$ channels.
- High driving forces ($F_x^* = 5.0$) result in flux values that are outside the experimental values and may correspond to local superheating or evaporation conditions.

The log-log type figure (Fig. 13) shows a summary of the ranges of water mass flux in nanochannels, obtained from our own computer simulations and from experimental and computational data available in the literature. The ordinate axis shows the mass flux values in log-log terms. The range of values obtained from our own computer simulations and from experimental and computational data available in the literature is indicated by vertical error bars, representing the span from the minimum to the maximum reported mass flux. The results obtained in this work (for $F_x^* = 0.5\text{--}2.5$) are in the same order of magnitude as experimental and computational data from the literature, confirming their physical plausibility.

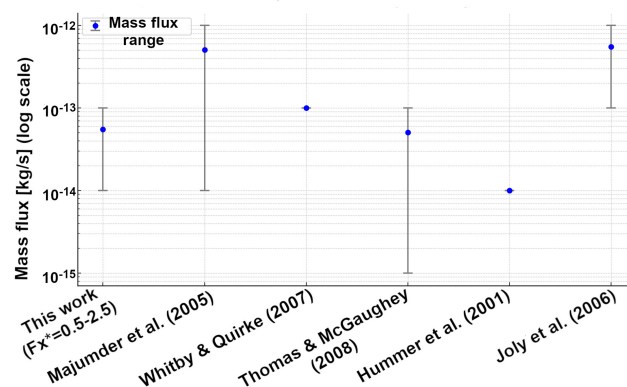


Fig. 13. Comparison of water mass flux in nanoflows (simulation results vs Experiment [19–23])

Table 3

Comparison of water mass flux in nanoflows: this study vs. experimental data [19–23]

Source / Conditions	Method / Configuration	Average mass flux (kg/s)	Notes
This work ($F_x^* = 0.5\text{--}2.5$)	MD, 60 water molecules, copper nanochannel	$\sim 10^{-14}\text{--}10^{-13}$ (estimated from the velocity distribution)	Values obtained from the average V_x^* distributions and the approximate water density in the nanochannel
Majumder <i>et al.</i> (<i>Nature</i> , 2005)	CNT (nanotubes), $\sim 7\text{ nm}$ diameter, different ΔP	$10^{-14}\text{--}10^{-12}$	Very high slippage observed, even 104 times greater than the classic one
Whitby & Quirke (<i>Nat. Nano.</i> 2007)	Graphene and oxide channels, nano-PIV	$\sim 10^{-13}$	Higher flow for hydrophobic walls
Thomas & McGaughey (<i>Nano Letters</i> , 2008)	MD, nanochannel SiO_2 and Cu, $\sim 5\text{ nm}$, TIP4P	$10^{-15}\text{--}10^{-13}$	Simulation data scaled to experimental values
Hummer <i>et al.</i> (<i>Nature</i> , 2001)	MD, water flow through CNT (0.8 nm)	$\sim 10^{-14}$	Flow induced by chemical potential difference
Joly <i>et al.</i> (<i>Phys. Rev. Lett.</i> , 2006)	Micro-PIV, Si nanochannels, 10–50 nm	$\sim 10^{-13}\text{--}10^{-12}$	Measured volumetric and mass flow rates

4. CONCLUSIONS

This work investigated the influence of externally applied forcing on water flow in a copper nanochannel using molecular dynamics and three molecular water models (OPC, PPC, TIP4P). The results demonstrate that the magnitude of the applied force critically determines the thermodynamic stability of the system. Only intermediate forcing values preserve the liquid phase and produce stable velocity distributions. Excessive forcing results in a rapid temperature increase leading to vaporization, while insufficient forcing promotes cooling that may induce solidification. The variation in response observed among the water models confirms that molecular model selection significantly affects nanoscale flow characteristics and cannot be disregarded when defining simulation parameters.

The simulations were performed for relatively small systems (60 and 280 molecules), which may limit the possibility of direct generalization of the results to real technical systems. Although the obtained trends were consistent for both sizes of systems, full scaling of the effects requires further studies. Popular water models (OPC, PPC, TIP4P) were used, which, despite their wide use in the literature, do not consider all the physicochemical properties of real water, such as quantum effects or polarization. In addition, the channel walls were modeled as perfectly ordered copper structures, free of defects and chemical interactions, which constitutes a simplification relative to real technological conditions, but it enables a clearer understanding of the fundamental transport mechanisms under idealized conditions and allows for an unambiguous interpretation of the effects of external forces and channel geometry without interference from uncontrollable material heterogeneities.

The study thus identifies a limited and well-defined forcing interval that enables physically consistent water flow at the nanoscale. The presented findings provide a basis for selecting appropriate simulation conditions and may facilitate the design of nanoscale systems in which stable liquid transport is required. Examples of applications include nanoporous materials, biosensors, and cooling systems in nanoscale devices.

REFERENCES

- [1] F. Ercolessi, *A molecular dynamics primer*. Triest: International School for Advanced Studies, 1997.
- [2] C. Zhuo, C. Zeng, H. Liu, H. Wang, Y. Peng, and Y. Zhao, "Advances and Mechanism of RNA – Ligand Interaction Predictions," *Life*, vol. 15, p. 104, 2025, doi: [10.3390/life15010104](https://doi.org/10.3390/life15010104).
- [3] S. Kazanc and C.A. Canbay, "Investigation of Bauschinger effect in single and polycrystalline bulk Au with molecular dynamics simulation," *Mol. Simul.*, vol. 51, pp. 104–114, 2025, doi: [10.1080/08927022.2025.2465783](https://doi.org/10.1080/08927022.2025.2465783).
- [4] A. Słowicka and Z. Walenta, "Formation of nanostructures in emulsions," *Systems*. vol. 11, no. 1, pp. 255–267, 2006.
- [5] M.S. Liu, B.D. Todd, and R.J. Sadus, "A mechanochemical theory for the ATP-fuelled biomolecular motors," *Int. J. Nanotechnol.*, vol. 6, no. 12, pp. 1121–1130, 2009, doi: [10.1504/IJNT.2009.028468](https://doi.org/10.1504/IJNT.2009.028468).
- [6] A.K. Singhal, "Key Elements of Verification and Validation of CFD Software," *29-th AIAA Fluid Dynamics Conference*, Albuquerque, USA, 1998, doi: [10.2514/6.1998-2639](https://doi.org/10.2514/6.1998-2639).
- [7] D. Frenkel and B. Smit, *Understanding Molecular Simulation*. London: Academic Press, 2002, doi: [10.1016/B978-0-12-267351-1.X5000-7](https://doi.org/10.1016/B978-0-12-267351-1.X5000-7).
- [8] M. Chaplin, "Water Structure and Science," *Water Models*. [Online] Available: https://water.lsbu.ac.uk/water/water_models.html [Accessed: Apr. 2024].
- [9] A. Kulkarni, M. Bortz, K.H. Küfer, M. Kohns, and H. Hasse, "Hierarchical Multicriteria Optimization of Molecular Models of Water," *J. Chem. Inf. Model.*, vol. 64, pp. 5077–5089, 2024, doi: [10.1021/acs.jcim.4c00404](https://doi.org/10.1021/acs.jcim.4c00404).
- [10] A. Kucaba-Piętal, "Molecular dynamics computer simulation of water flows in nanochannels," *Bull. Pol. Acad. Sci. Tech. Sci.*, vol. 57, no. 1, pp. 55–61, 2009, doi: [10.2478/v10175-010-0105-4](https://doi.org/10.2478/v10175-010-0105-4).
- [11] G. Karniadakis, A. Beskok and N. Aluru, *Microflows and Nanoflows*. New York: Springer, 2005, doi: [10.1007/0-387-28676-4](https://doi.org/10.1007/0-387-28676-4).
- [12] P. Schwerdtfeger and D.J. Wales, "100 Years of the Lennard-Jones Potential," *J. Chem. Theory Comput.*, vol. 20, pp. 3379–3405, 2024, doi: [10.1021/acs.jctc.4c00135](https://doi.org/10.1021/acs.jctc.4c00135).
- [13] K. Refson, "Moldy User's Manual," Department of Earth Sciences, Oxford, 2001. [Online] Available: <http://www.ccl.net/cca/software/SOURCES/C/moldy/moldy-manual.pdf> [Accessed: Apr. 2024].
- [14] A.J. Iwasaki, M. Kirsz, C.G. Pruteanu, and G.J. Ackland, "An Accurate Machine-Learned Potential for Krypton under Extreme Conditions," *J. Phys. Chem. Lett.* vol. 16, pp. 1559–1566, 2025, doi: [10.1021/acs.jpcclett.4c03272](https://doi.org/10.1021/acs.jpcclett.4c03272).
- [15] B.P. Akhouri and J.R. Solana, "Equilibrium thermodynamic properties of Lennard–Jones fluid mixtures from a single-component effective fluid model," *Mol. Simul.*, vol. 49, pp. 1117–1124, 2023, doi: [10.1080/08927022.2023.2219751](https://doi.org/10.1080/08927022.2023.2219751).
- [16] A. Kucaba-Piętal, *Microflows modelling by use micropolar fluid model*, Oficyna Wydawnicza Politechniki Rzeszowskiej, Rzeszów, 2004.
- [17] B.J. Adler: "Molecular Dynamics Simulations of Copper using Moldy," Cornell University, 2003, [Online] Available: <https://reu.magnet.fsu.edu/program/2003/paper/adler.doc>
- [18] J.H. Walther and P. Koumoutsakos, "Molecular dynamics simulation of nanodroplet evaporation," *J. Heat Transfer*, vol. 123, pp. 741–748, 2001, doi: [10.1115/1.1370517](https://doi.org/10.1115/1.1370517).
- [19] M. Whitby and N. Quirke, "Fluid flow in carbon nanotubes and nanopipes" *Nature Nanotech.*, vol. 2, pp. 87–94, 2007, doi: [10.1038/nnano.2006.175](https://doi.org/10.1038/nnano.2006.175).
- [20] M. Majumder, N. Chopra, R. Andrews and B.J. Hinds, "Enhanced flow in carbon nanotubes," *Nature*, vol. 438, p. 44, 2005, doi: [10.1038/438044a](https://doi.org/10.1038/438044a).
- [21] J.A. Thomas and A.J. McGaughey, "Reassessing fast water transport through carbon nanotubes" *Nano Lett.*, vol. 8, no. 9, pp. 2788–2793, 2008, doi: [10.1021/nl8013617](https://doi.org/10.1021/nl8013617).
- [22] G. Hummer, J. Rasaiah, and J. Noworyta, "Water conduction through the hydrophobic channel of a carbon nanotube" *Nature*, vol. 414, pp. 188–190, 2001, doi: [10.1038/35102535](https://doi.org/10.1038/35102535).
- [23] L. Joly, C. Ybert, and L. Bocquet, "Probing the nanohydrodynamics at liquid-solid interfaces using thermal motion," *Phys. Rev. Lett.*, vol. 96, p. 046101, 2006, doi: [10.1103/PhysRevLett.96.046101](https://doi.org/10.1103/PhysRevLett.96.046101).